MAXIMUM POWER POINT TRACKING FOR PHOTOVOLTAIC OPTIMIZATION USING EXTREMUM SEEKING

Steven L. Brunton[1], Clarence W. Rowley[1], Sanjeev R. Kulkarni[1], and Charles Clarkson[2]
[1]Princeton University, Princeton, NJ 08544
[2]ITT Space Systems Division, Rochester, NY 14606

ABSTRACT

This work develops a maximum power point tracking (MPPT) algorithm for optimizing solar array performance that is robust to rapidly varying weather conditions. In particular, a novel extremum seeking (ES) controller, which utilizes the inverter ripple, is designed and tested on a simulated array with grid-tied inverter. The new algorithm is benchmarked against the perturb and observe (PO) method using irradiance data gathered on a rooftop array experiment in Princeton, NJ. The extremum seeking controller achieves an efficiency of 99.7% and transient rise to the MPP of .1 seconds, which is 100 times faster than perturb and observe.

INTRODUCTION

Solar power is at the forefront of clean, renewable energy, and it is gaining momentum due to advances in solar panel manufacturing and efficiency as well as increasingly volatile fuel costs. Photovoltaic (PV) solar cells are the most readily available solar technology, and they operate best on bright days with little or no obstruction to incident sunlight. However, frequent overcast days and partial obstructions such as tree limbs or buildings limit the reliability of solar power in much of the United States.

Because of the photovoltaic nature of solar panels, their current-voltage, or IV, curves depend on temperature and irradiance levels [1]. Therefore, the operating current and voltage which maximize power output will change with environmental conditions, as in Figure 1. There are a number of maximum power point tracking (MPPT) algorithms which track the optimal current and voltage in a changing environment [2]. A grid-tied inverter is able to draw at a specified command current on-the-fly, providing the control authority necessary to design and apply MPPT algorithms even in rapidly changing weather.

Control algorithms which are not based on a particular model and are robust to uncertain system parameters are ideal for a number of reasons. Fewer sensors are necessary to reconstruct the state, and the system requires less frequent maintenance for fine tuning. Moreover, robust, model independent algorithms are applicable to a wide range of panel and inverter technologies. There are a number of "black box" MPPT algorithms, such as perturb and observe and incremental conductance [2], but each has drawbacks in terms of convergence rates and stability. The extremum seeking method of Krstic [3] offers the best of both worlds with fast convergence and guaranteed stability over a range of conditions.

This work is motivated by the need to optimize solar array performance in New Jersey's climate, which is characterized by rapidly varying environmental conditions. The grid-tied inverter is currently the most efficient device to bring solar power into the grid, with efficiencies reaching 95%. A local company, Princeton Power, is scaling down their commercial inverters for testing on a 3kW solar array on the roof of Princeton's engineering quad, shown in Figure 2. The array consists of two advanced PV solar technologies, GE's hard poly-crystalline silicon panels and EPV's amorphous silicon thin films; EPV is a local solar panel manufacturer. The solar array aims to supply the power consumed by an average home in New Jersey.

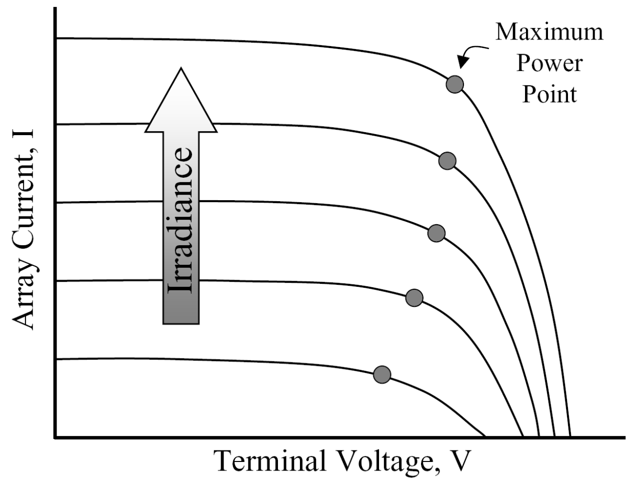

Fig. 1. IV curves at various irradiance.

Fig. 2. Two solar arrays at Princeton University.

PV ARRAY INVERTER MODEL

Figure 3 is a schematic of the array-inverter system.

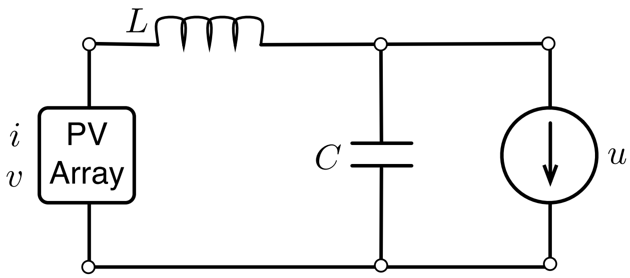

Fig. 3. Schematic of PV array and inverter with LC dynamics.

Kirchoff's law yields the following relationships:

$$i = u + i_C \tag{1}$$
$$v_C = -v - v_L \tag{2}$$

The array IV curve has the form $v = f(i, G)$, where G is irradiance, so equation (2) becomes:

$$v_C = -f(i, G) - L\frac{di}{dt} \tag{3}$$
$$\implies -\frac{dv_C}{dt} = \frac{d}{dt}f(i, G) + L\frac{d^2 i}{dt^2} \tag{4}$$
$$= \frac{\partial f(i, G)}{\partial i}\frac{di}{dt} + \frac{\partial f(i, G)}{\partial G}\frac{dG}{dt} + L\frac{d^2 i}{dt^2} \tag{5}$$

Equation (1) and the capacitor equation yield:

$$\frac{dv_C}{dt} = \frac{i_C}{C} \implies \frac{dv_C}{dt} = -\frac{1}{C}(u - i) \tag{6}$$

Combining equations (5) & (6) yields the system dynamics in terms of inverter control current u and array current i:

$$LC\frac{d^2 i}{dt^2} + C\frac{\partial f}{\partial i}\frac{di}{dt} + i = u - C\frac{\partial f}{\partial G}\frac{dG}{dt} \tag{7}$$

The dynamical system given by equation (7) represents a forced oscillator with nonlinear damping. The forcing corresponds to the inverter control current u as well as the change in IV curve due to irradiance change, given by $-C(\partial f/\partial G)(dG/dt)$.

To flow 60Hz AC power into the grid at a given current $\hat{u}$, the inverter switches DC current out of a large capacitor. This requires the following inverter control current with a large 120Hz oscillation:

$$u = \hat{u}\,(1 + \sin(120 \times 2\pi t)) \tag{8}$$

In practice, the LC circuit acts as a low pass filter between the control current u, and the array current i, so that i experiences a 120Hz ripple at approximately 3% magnitude:

$$i \approx \hat{u}\,(1 + .03\sin(120 \times 2\pi t + \varphi)) \tag{9}$$

For more information on DC-AC power inverters, see Bose [4].

There is also a high frequency ripple at 20kHz due to the inverter sampling time; however, this is a small effect and is not modeled.

The array IV curve $v = f(i, G)$ is modeled using the lighted-diode equations [1], [5]:

$$I = I_L - I_{OS}\left[\exp\frac{q}{Ak_BT}(V + IR) - 1\right] \tag{10}$$
$$I_{OS} = I_{OR}\left(\frac{T}{T_R}\right)\exp\left(\frac{qE_G}{Ak_B}\left(\frac{1}{T_R} - \frac{1}{R}\right)\right) \tag{11}$$
$$I_L = \frac{G}{1000}(I_{SC} + K_{T,I}(T - T_R)) \tag{12}$$
$$V = \frac{Ak_BT}{q}\ln\left(\frac{I_L - I}{I_{OS}} + 1\right) - IR \tag{13}$$

where I and V are the same as i, v in Figure 3, I_L is the light generated current, I_{OS} is the cell reverse saturation current, and T is temperature.

Values and definitions for other terms in the equations are as follows: $T_R = 298$ (reference temperature), $I_{OR} = 2.25e-6$ (reverse saturation current at $T = T_R$), $I_{SC} = 3.2$ (short-circuit current), $E_G = 1.8e-19$ (Silicon band gap), $A = 1.6$ (ideality factor), $k_B = 1.38e-23$ (Boltzmann's constant), $q = 1.6e-19$ (electronic charge), $R = .01$ (resistance), and $K_{T,I} = .8$ (short-circuit current temperature coefficient). Finally, the model array consists of 3 parallel strings, each with 7 panels connected in series. Each panel produces approximately $220W$ at full irradiance, $G = 1000\ W/m^2$.

MAXIMUM POWER POINT TRACKING

Currently the most popular MPPT algorithm is perturb and observe (PO), where the current is repeatedly perturbed by a fixed amount in a given direction, and the direction is changed only if the algorithm detects a drop in power between steps. Although this algorithm benefits from simplicity, it lacks the speed and adaptability necessary for tracking fast transients in weather.

A robust new maximum power point tracking algorithm is based on the extremum seeking (ES) control method. A schematic of the algorithm is shown in Figure 4. This controller converges at a rate which is proportional to the slope of the PI curve and has guaranteed stability over a range of system parameters [3].

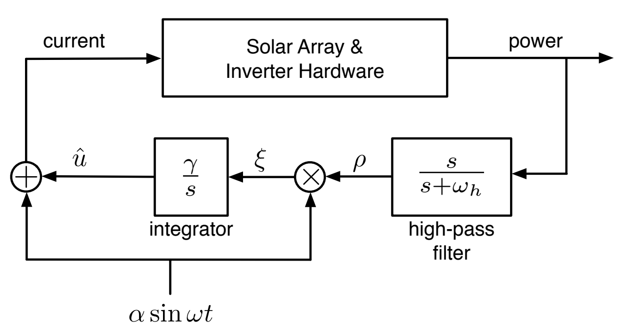

Fig. 4. Extremum seeking algorithm.

In practice, rather than injecting a sinusoidal control perturbation $\alpha \sin \omega t$, as in the standard extremum seeking algorithm, it is convenient to utilize the inverter ripple for the perturbation. Thus, by using the control signal in equation (8), the array current and power will have a small ripple, as in equation (9). Finally, the high-pass filtered array current and power are multiplied, yielding the demodulated signal, ξ, similar to Figure 4.

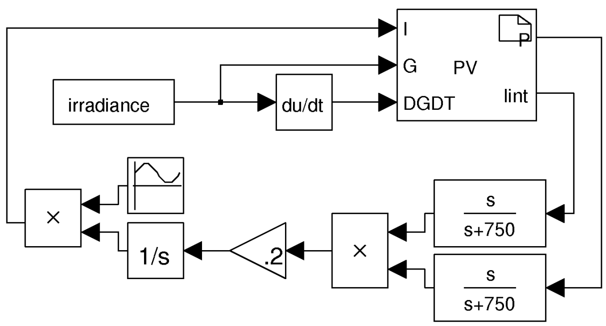

Fig. 5. Extremum seeking algorithm utilizing array/inverter ripple.

RESULTS

Figure 6 shows irradiance data for two consecutive days in June, 2007. The data was gathered on the Princeton University solar deck. The experiments below simulate operation using 25 minutes of measured irradiance data from 12:34-12:59AM on June 20th, 2007 (day 2). This time period is chosen because it includes rapid irradiance changes as a result of scattered cloud cover. Moreover, choosing a short 25 minute window makes it easier to see the controller response to individual irradiance changes.

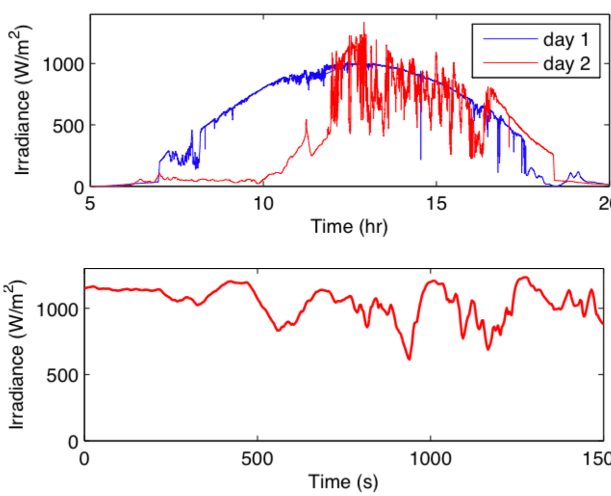

Fig. 6. (top) Irradiance data for two days in June in Princeton, NJ. (bottom) Irradiance data spanning 25 minutes from 12:34-12:59AM on June 20th, 2007. Signal is low-pass filtered, so that noisy data is averaged over about 10 seconds.

Using the irradiance data as an input to the model, both the extremum seeking (ES) and perturb and observe (PO) algorithms were tested using MATLAB®/Simulink models [6], [7]. The extremum seeking model is shown in Figure 5. The incremental step used for perturb and observe is $.5A$ at discrete time steps of $\Delta t = .1s$, with 1kHz power sampling.

Figure 7 shows the array power and current vs. time for ES (blue), PO (green), and the true maximum power (red). The extremum seeking method commands a control current which oscillates more closely around the true maximum power current, as seen in the bottom plot. Power is integrated over the 25 minute period to compute efficiency as a percentage of maximum power possible. Perturb and observe is 98.8% efficient, while extremum seeking is 99.7% efficient.

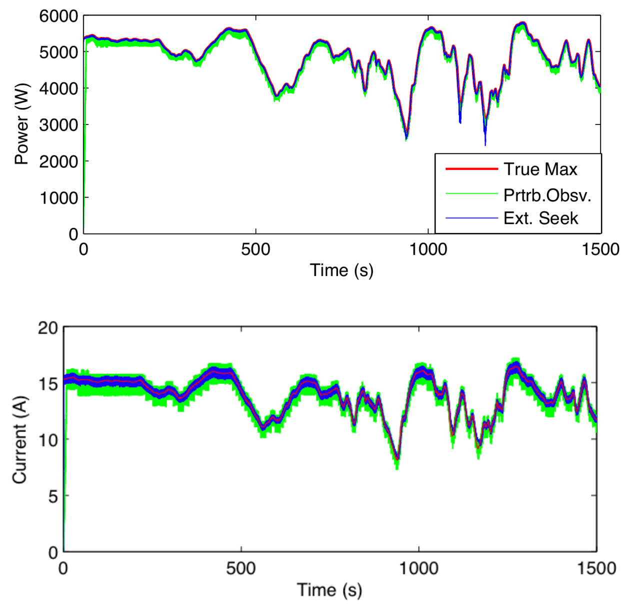

Fig. 7. (top) Array power vs time. (bottom) Array current vs time; comparison of true maximum (red), ES (blue), and PO (green).

To achieve comparable tracking performance, the incremental step for perturb and observe is large, $\Delta i = .5A$. Two disadvantages are additional stress on the system components as well as a poorer performance about the maximum power point, shown in Figure 8.

Finally, the transient rise time to the maximum power point is much slower for perturb and observe compared with extremum seeking. Figure 9 shows the transient rise to the maximum power point, which takes extremum seeking $.1$ seconds and perturb and observe 10 seconds. Rise time is especially important if the irradiance drops so rapidly that the control current cannot compensate and passes through the short circuit current. In this case, the inverter is stalled, and the algorithm will need to re-track the maximum power point.

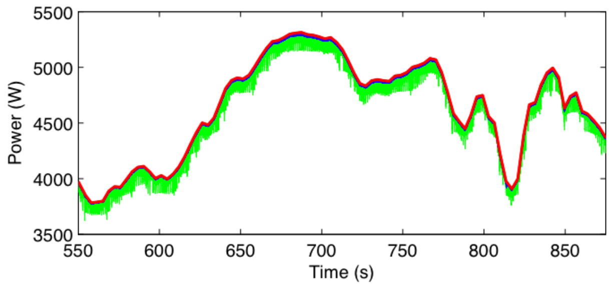

Fig. 8. Array power vs. time; PO (green) has larger tracking error than ES (blue).

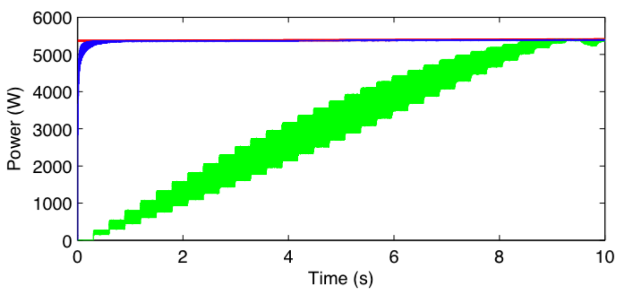

Fig. 9. Transient rise to maximum power point as controller is turned on. ES (blue) rises in .1 seconds, while PO (green) rises in 10 seconds.

CONCLUSIONS

A novel extremum seeking algorithm that utilizes the inverter ripple was tested on a simulated array-inverter system using MATLAB®/Simulink. This method was benchmarked against the popular perturb and observe method using 25 minutes of rapidly varying irradiance data taken in June, 2007 on the Princeton University solar deck. The irradiance data chosen represents a worst-case scenario for maximum power point tracking due to the presence of fast moving, scattered cloud cover. It was shown that extremum seeking slightly outperforms perturb and observe in total power efficiency, and drastically outperforms in transient rise-time to the maximum power point, with two orders of magnitude speed-up. Additionally, extremum seeking has guaranteed convergence and stability properties which are ideal for variable weather conditions and unmodeled dynamics.

It remains to test the algorithms on the actual solar array at Princeton University. Additionally, it would be interesting to compare the algorithms on competing photovoltaic technologies, namely GE poly-crystalline silicon panels and EPV's amorphous silicon thin films, to see how the shape of the panel IV curve affects tracking performance. Here, only irradiance variations were considered, although temperature and partial shading experiments would also be interesting. Finally, a next step is to extend the extremum seeking algorithm to have a variable gain and compare with a modified perturb and observe algorithm with variable increment.

ACKNOWLEDGMENT

This work was supported by a grant from the New Jersey Commission on Science and Technology (NJCST) to optimize solar array performance in New Jersey. The authors would like to thank Mark Holveck, Erik Limpaecher, Swarnab Banerjee and Frank Hoffmann from Princeton Power Systems for assembling the rooftop solar array and data acquisition, as well as for helpful discussions about inverter models. We would also like to thank Loan Le and Alan Delahoy at EPV for helpful discussions on solar panel characteristics.

REFERENCES

[1] K. Hussein, I. Muta, T. Hoshino, and M. Osakada, "Maximum Photovoltaic Power Tracking: An Algorithm for Rapidly Changing Atmospheric Conditions", *IEEE Proceedings. Generation, Transmission and Distribution,* 1995, **142**, (1), pp. 59-64

[2] D. Hohm and M. Ropp, "Comparative Study of Maximum Power Point Tracking Algorithms", *Progress in Photovoltaics: Research and Applications,* 2003, **11**, pp. 47-62

[3] M. Krstic, "Extremum Seeking Control for Discrete-Time Systems", *IEEE Transactions on Automatic Control,* 2002, **47**, (2), pp. 318-323

[4] B.K. Bose, *Modern Power Electronics: Evolution, Technology, and Applications.* New York: IEEE Press, 1992.

[5] G. Vachtsevanos and K. Kalaitzakis, "A Hybrid Photovoltaic Simulator for Utility Interactive Studies", *IEEE Transactions on Energy Conversion,* 1987, **EC-2**, (2), pp. 227-231

[6] Matlab - the language of technical computing. "Using MATLAB, 6th.", Natick: The Mathworks Inc.; 2001.

[7] Simulink - model-based and system-based design. "Using Simulink, 4th.", Natick: The Mathworks Inc.; 2001.